Polymorphic transitions in single crystals: A new molecular dynamics method

M. Parrinello and A. Rahman

Citation: Journal of Applied Physics **52**, 7182 (1981); doi: 10.1063/1.328693
View online: http://dx.doi.org/10.1063/1.328693
View Table of Contents: http://scitation.aip.org/content/aip/journal/jap/52/12?ver=pdfcov
Published by the AIP Publishing

Polymorphic transitions in single crystals: A new molecular dynamics method

M. Parrinello
University of Trieste, Trieste, Italy

A. Rahman
Argonne National Laboratory, Argonne, Illinois 60439

(Received 1 July 1981; accepted for publication 14 August 1981)

A new Lagrangian formulation is introduced; it can be used to make molecular dynamics (MD) calculations on systems under the most general, externally applied, conditions of stress. In this formulation the MD cell shape and size can change according to dynamical equations given by this Lagrangian. This new MD technique is well suited to the study of structural transformations in solids under external stress and at finite temperature. As an example of the use of this technique we show how a single crystal of Ni behaves under uniform uniaxial compressive and tensile loads. This work confirms some of the results of static (i.e., zero temperature) calculations reported in the literature. We also show that some results regarding the stress-strain relation obtained by static calculations are invalid at finite temperature. We find that, under compressive loading, our model of Ni shows a bifurcation in its stress-strain relation; this bifurcation provides a link in configuration space between cubic and hexagonal close packing. It is suggested that such a transformation could perhaps be observed experimentally under extreme conditions of shock.

PACS numbers: 64.70.Kb, 61.50.Ks

I. INTRODUCTION

The behavior of solids under the combined effects of external stress and of temperature has considerable practical relevance. Yet even in the idealized case of a perfect crystal, a detailed microscopic picture of such effects is still lacking. Most of the theoretical studies have been confined to conditions at zero temperature; in addition a perfect and prefixed crystalline arrangement of the atoms has been assumed. These two assumptions may lead to useful insights for relatively small values of the stress and temperature. However, it is obviously desirable to be able to study the behavior of solids at normal temperatures and high levels of external stress. In particular at high values of the stress spontaneous defect generation and/or crystal structure transformation become possible; this makes the assumption of a perfect, even if elastically distorted, crystalline arrangement untenable. Furthermore, these processes are sensitive to temperature variations as well.

The experience of the past two decades has shown that molecular dynamics (MD) calculations can provide a valuable tool to investigate nonharmonic effects in solids.[1] The authors have recently developed[2] a new MD method which allows a crystalline system to modify its structure if the temperature and external stress conditions make such a modification favorable. This method is therefore pertinent to the discussion of stress and temperature effects just mentioned above.

It is our purpose to present work based on this new MD method; the model system which we have studied has been described in a series of papers by Milstein and collaborators.[3–5] It is a system of classical particles interacting via a pairwise additive potential of the Morse type. The parameters of the potential have been adjusted to reproduce the elastic constants and the lattice parameter of Ni.[3] We have used this model of Ni for our study. The significance of the results for laboratory experiments will be dealt with in the last section.

Two reasons have prompted our interest in this model. First, Milstein and collaborators[3–5] have made extensive calculations of stress-strain relations for this model of Ni. Their calculations are a convenient check for our method of calculation at least for those values of temperature and stress where their theoretical approach is expected to be valid.

Second, in a recent paper an interesting possibility has been suggested by Milstein and Farber.[5] They have considered an fcc crystal of Ni under a uniform tensile [100] load. As the load is increased the crystal stretches in the direction of the load and contracts in the lateral directions. Beyond a certain value of the load and hence of the extension in the [100] direction, a new path in the stress-strain relation becomes possible along which the tetragonal symmetry is broken. Along this new branch, with *decreasing* load, the system starts to *expand* in one of the two lateral directions and eventually its extension in that lateral direction "catches up" with the [100] extension, the system ending up, at zero load, again in a tetragonal face-centered structure.

We show here that at finite temperature the above-mentioned "bifurcation" does not occur. Instead very close to the bifurcation point the system actually fails. Moreover the zero load tetragonal face-centered states (except the fcc one) mentioned in Ref. 5 as possible stable states spontaneously evolve into an hcp structure even at very low temperature.

A new result we have found is that, for this model of Ni, upon uniform uniaxial compression, the fcc structure transforms into an hcp arrangement.

II. MOLECULAR DYNAMICS AT CONSTANT EXTERNAL STRESS

Molecular dynamics (MD) methods have been exten-

 0021-8979/81/127182-09$01.10

sively used in the past to study a variety of physical systems; for a detailed description the reader is referred to the book by Hansen and McDonald.[6] However, for the sake of clarity we shall briefly review the main features of MD.

It is a method for studying classical statistical mechanics of well-defined systems through a numerical solution of Newton's equations. A set of N classical particles have coordinates $\mathbf{r}_i$, velocities $\dot{\mathbf{r}}_i$ and masses $m_i, i = 1,...,N$. The particles interact through a potential $V_N(\mathbf{r}_1,...,\mathbf{r}_N)$ which, in most investigations is taken to be:

$$V_N = \frac{1}{2}\sum_i\sum_j \phi(r_{ij}), \tag{2.1}$$

where $r_{ij} = |\mathbf{r}_{ij}| = |\mathbf{r}_i - \mathbf{r}_j|$. More general forms of V_N can also be used, perhaps at the cost of more computational labor. Newton's equations are then

$$m_i\ddot{\mathbf{r}}_i = \sum_{j\neq i}\frac{1}{r_{ij}}\frac{d\phi}{dr_{ij}}\mathbf{r}_{ij}, \quad i = 1,...,N, \tag{2.2}$$

and are solved numerically. As the system evolves in time it eventually reaches equilibrium conditions in its dynamical and structural properties; the statistical averages of interest are calculated from $\mathbf{r}_i(t)$ and $\dot{\mathbf{r}}_i(t), i = 1,...,N$, as temporal averages over the trajectory of the system in its phase space. For practical reasons N is restricted to at most a few thousand and for small systems surface effects are obviously very important. However, to simulate a bulk system the common practice is to use periodic boundary conditions. These are obtained by periodically repeating a unit cell of volume Ω containing the N particles by suitable translations. Periodic boundary conditions obviously give a system in which the N particles are always contained in a cell of volume Ω, and without loss of generality every particle can be thought of as being at the "center." In other words, the summation over j in Eq. (2.2) extends over the infinite system generated by the periodic boundary conditions.

As a consequence of V_N being a function of $\mathbf{r}_i$ only [Eq. (2.1)], the solution of Eq. (2.2) conserves the total energy E of the system; thus the statistical ensemble generated in a conventional MD calculation is a (Ω,E,N) ensemble or a microcanonical ensemble. We shall use (.....) to indicate quantities whose constancy characterizes a given statistical ensemble.

The restriction that the MD cell be kept constant in volume and in shape severely restricts the applicability of the method to problems involving crystal structure transformations; in such transformations changes in the shape of the cell most obviously play an essential role. (For example, in a plane four points at the vertices of a square together with one at the center can obviously be used to generate a square lattice of points; this can become a lattice of equilateral triangles only if the square is allowed to become a $1:\sqrt{3}$ rectangle.)

In order to overcome this difficulty we[2] have modified a method due to Andersen[7] so as to allow for changes in volume *and* shape of the MD cell containing a system of particles under constant external hydrostatic pressure. Note that in the method of Andersen[7] only changes in the volume of the MD cell were possible but not in its shape. Thus crystal structure transformations are inhibited in Andersen's method because of the suppression of the essential fluctuations, namely those in the shape of the MD cell.

This extra degree of flexibility was introduced into the MD method as follows[2]: As before the system consists of N particles in a cell that is periodically repeated to fill all space. However, the cell can have arbitrary shape and volume being completely described by three vectors **a**, **b**, and **c** that span the edges of the MD cell. The vectors **a**, **b**, and **c** can have different lengths and arbitrary mutual orientations. An alternative description is obtained by arranging the vectors as $\{\mathbf{a}, \mathbf{b}, \mathbf{c}\}$ to form a 3×3 matrix $\mathbf{h}$ whose columns are, in order, the components of **a**, **b**, and **c**. The volume is given by

$$\Omega = \|\mathbf{h}\| = \mathbf{a}\cdot(\mathbf{b}\wedge\mathbf{c}); \tag{2.3}$$

a, **b**, and **c**, in that order, are assumed to be a right-handed triad.

The position $\mathbf{r}_i$ of a particle i can be written in terms of $\mathbf{h}$ and of a column vector $\mathbf{s}_i$, with components ξ_i,η_i, and ζ_i, as

$$\mathbf{r}_i = \mathbf{h}\mathbf{s}_i = \xi_i\mathbf{a} + \eta_i\mathbf{b} + \zeta_i\mathbf{c}. \tag{2.4}$$

Obviously $0\leqslant\xi_i,\eta_i,\zeta_i\leqslant 1$ is the range of variation of the numbers $\xi_i,\eta_i,\zeta_i, i = 1,...,N$. The images of $\mathbf{s}_i$ are at $\mathbf{s}_i + (\lambda,\mu,\nu)$ where λ, μ, and ν are integers from $-\infty$ to $+\infty$.

Let a prime $'$ denote a transpose of a vector or a tensor in the usual way. Then the square of the distance between i and j is given by

$$r_{ij}^2 = (\mathbf{s}_i - \mathbf{s}_j)'\mathbf{G}(\mathbf{s}_i - \mathbf{s}_j), \tag{2.5}$$

where the metric tensor $\mathbf{G}$ is

$$\mathbf{G} = \mathbf{h}'\mathbf{h}. \tag{2.6}$$

To complete the notation used here we note finally that the reciprocal space is spanned by the vectors

$$\frac{2\pi}{\Omega}\{\mathbf{b}\wedge\mathbf{c},\mathbf{c}\wedge\mathbf{a},\mathbf{a}\wedge\mathbf{b}\} \equiv \frac{2\pi}{\Omega}\boldsymbol{\sigma}. \tag{2.7}$$

The matrix $\boldsymbol{\sigma}\equiv\Omega\mathbf{h}'^{-1}$, carries information concerning the size and orientation of the MD cell.

A. The case when only hydrostatic pressure is applied

In Ref. (2) variability in the shape and size of the MD cell was obtained as follows: the usual set of $3N$ dynamical variables, that describe the positions of the N particles, was augmented by the nine components of $\mathbf{h}$. The time evolution of the $3N + 9$ variables was then obtained from the Lagrangian

$$\mathscr{L} = 1/2\sum_{i=1}^{N} m_i\dot{\mathbf{s}}_i'\mathbf{G}\dot{\mathbf{s}}_i - \sum_{i=1}^{N}\sum_{j>i}^{N}\phi(r_{ij}) + 1/2W\,\mathrm{Tr}\,\dot{\mathbf{h}}'\dot{\mathbf{h}} - p\Omega, \tag{2.8}$$

where p is the hydrostatic pressure that we intended to impose on the system. We shall comment later on W, which has dimensions of mass. Whether such a Lagrangian is derivable from first principles is a question for further study; its validity can be judged, as of now, by the equations of motion and the statistical ensembles that it generates. From Eq. (2.8) the equations of motion are easily found. We get

$$\ddot{\mathbf{s}}_i = -\sum_{j\neq i} m_i^{-1}(\phi'/r_{ij})(\mathbf{s}_i - \mathbf{s}_j) - \mathbf{G}^{-1}\dot{\mathbf{G}}\dot{\mathbf{s}}_i, i = 1,...,N, \tag{2.9}$$

$$W\ddot{\mathbf{h}} = (\boldsymbol{\pi} - p)\boldsymbol{\sigma}, \tag{2.10}$$

where, using the usual dyadic notation, and writing $\mathbf{v}_i = \mathbf{h}\dot{\mathbf{s}}_i$,

$$\Omega\boldsymbol{\pi} = \sum_i m_i \mathbf{v}_i \mathbf{v}_i - \sum_i \sum_{j>i} (\phi'/r_{ij}) \mathbf{r}_{ij} \mathbf{r}_{ij}. \tag{2.11}$$

When $\mathbf{h}$ = constant, i.e., when the MD cell is time independent, $\dot{\mathbf{G}} = 0$, and due to Eq. (2.4), Eq. (2.9) becomes identical to Eq. (2.2). Of course the pressure in the system cannot be controlled; its value can be obtained from 1/3 of the trace of the average of $\boldsymbol{\pi}$ in the usual way.

The equations derived by Hoover *et al.*[8] have a close affinity with Eq. (2.9) above. Their two first-order equations of motion are equivalent to Eq. (2.9) on identifying $\dot{\mathbf{h}}\mathbf{h}^{-1}$ with their strain rate tensor transpose. Thus $\dot{\mathbf{h}}$ = (strain-rate tensor)$'\mathbf{h}$ and hence, as desired by them, $\mathbf{h}$ is driven by the strain-rate tensor. Their equations are thus suitable for the study of externally driven nonequilibrium phenomena.

Equation (2.10), however, allows the system to be driven by the dynamic imbalance between the externally applied stress and the internally generated stress tensor [the more general case is given in Eq. (2.25) below]; thus Eq. (2.10) allows one to study nonequilibrium phenomena driven by the above mentioned imbalance. In a state of equilibrium, making the external stress have an oscillatory time dependance will also allow one to study frequency dependent response of the system to external stimuli of various kinds. From Eq. (2.10) it also follows that the mass W determines the relaxation time for recovery from an imbalance between the external pressure and the internal stress. As discussed by Andersen[7], an appropriate choice for the value of W can make this relaxation time of the same order of magnitude as that of the relaxation of a small portion of a much larger sample. His suggestion is for a choice of W such that the above-mentioned relaxation time is of the same order of magnitude as the time L/c, where L is the MD cell size and c is the sound velocity. This obviously eliminates the arbitrariness in the choice of W and makes the calculation more realistic. However, if one is interested only in static averages, W can be chosen on the basis of computational convenience. In fact, in classical statistical mechanics, the equilibrium properties of a system are independent of the masses of its constituent parts.

From Eq. (2.8) one can construct the corresponding Hamiltonian following the usual rules of mechanics. Since the system is not subject to time dependent external forces this is a constant of motion. We get

$$\mathscr{H} = \sum_i 1/2 m_i \mathbf{v}_i^2 + \sum_i \sum_{j>i} \phi(r_{ij}) + 1/2 W \operatorname{Tr} \dot{\mathbf{h}}'\dot{\mathbf{h}} + p\Omega. \tag{2.12}$$

In equilibrium, at temperature T, $9/2 k_B T$ is contributed by the term with W and $3N/2\, k_B T$ by the other kinetic terms. Therefore to an accuracy of $3{:}N$ one finds that the constant of motion $\mathscr{H}$ is nothing but the enthalpy

$$H = E + p\Omega, \tag{2.13}$$

where

$$E = \sum_i 1/2 m_i \mathbf{v}_i^2 + \sum_i \sum_{j>i} \phi(r_{ij}). \tag{2.14}$$

Hence the Lagrangian in Eq. (2.8) generates a (p, H, N) ensemble.[7]

B. The case when a general stress is applied

The above formulation of MD, briefly presented before,[2] lends itself quite naturally to the introduction of *nonisotropic* external stress. This is not difficult to realize since in the classical theory of elasticity the notion of strain is intimately connected to the variations in the metric tensor and, as has surely been noticed, $\mathbf{G}$ is a natural constituent of our MD scheme.

In order to make the above remark practicable, we need to introduce, as is usually done in elasticity theory,[9] a reference state. Using the notions already introduced, this reference state of the system can be defined by its matrix $\mathbf{h}_0$ and volume $\Omega_0 = \|\mathbf{h}_0\|$. In this reference state a point in space given by the coordinate vector $\mathbf{s}$ is at the position

$$\mathbf{r}_0 = \mathbf{h}_0 \mathbf{s}. \tag{2.15}$$

A homogeneous distortion of the system changes $\mathbf{h}_0$ to $\mathbf{h}$, moving $\mathbf{r}_0$ to $\mathbf{r}$ where

$$\mathbf{r} = \mathbf{h}\mathbf{s} = \mathbf{h}\mathbf{h}_0^{-1}\mathbf{r}_0, \tag{2.16}$$

giving the displacement $\mathbf{u}$ due to the distortion:

$$\mathbf{u} = \mathbf{r} - \mathbf{r}_0 = (\mathbf{h}\mathbf{h}_0^{-1} - 1)\mathbf{r}_0. \tag{2.17}$$

Following Landau and Lifshitz[9] to define the strain tensor $\boldsymbol{\epsilon}$, and using x_μ to denote the components of $\mathbf{r}_0$,

$$\epsilon_{\lambda\mu} = 1/2\left(\frac{\partial u_\lambda}{\partial x_\mu} + \frac{\partial u_\mu}{\partial x_\lambda} + \sum \frac{\partial u_\nu}{\partial x_\mu} \frac{\partial u_\nu}{\partial x_\lambda} \right), \tag{2.18}$$

we find, using Eq. (2.6) which defines $\mathbf{G}$ and Eq. (2.17) which defines $\mathbf{u}$, that

$$\boldsymbol{\epsilon} = 1/2\,(\mathbf{h}_0'^{-1}\mathbf{G}\mathbf{h}_0^{-1} - 1) \tag{2.19}$$

(We give in an appendix the connection between this formal definition of $\boldsymbol{\epsilon}$ in Eq. (2.19) and that given in elementary text books.)

Having identified the strain $\boldsymbol{\epsilon}$, an expression for the elastic energy, V_{el}, can now be written. If $\mathbf{S}$ is the external stress[10] and p the hydrostatic pressure,

$$V_{\text{el}} = p(\Omega - \Omega_0) + \Omega_0 \operatorname{Tr}(\mathbf{S} - p)\boldsymbol{\epsilon}. \tag{2.20}$$

In the limit of small strain,

$$\operatorname{Tr}\boldsymbol{\epsilon} \simeq \Delta\Omega/\Omega_0 = (\Omega - \Omega_0)/\Omega_0. \tag{2.21}$$

Hence, when Eq. (2.21) is a valid approximation, we get the more familiar expression,

$$V_{\text{el}} \simeq \Omega_0 \operatorname{Tr} \mathbf{S}\boldsymbol{\epsilon}. \tag{2.22}$$

Otherwise, i.e. when Eq. (2.21) is not valid, we need Eq. (2.20) to get the correct description of the effects of hydrostatic pressure.

To generalize the Lagrangian of Eq. (2.8) we need to substitute V_{el} of Eq. (2.20) in place of $p\Omega$ in Eq. (2.8) for $\mathscr{L}$. This gives us the new Lagrangian $\mathscr{L}_s$,

$$\mathscr{L}_s = \mathscr{L} - 1/2 \operatorname{Tr} \boldsymbol{\Sigma}\mathbf{G}, \tag{2.23}$$

where the symmetric tensor $\boldsymbol{\Sigma}$ is related to the stress $\mathbf{S}$:

$$\boldsymbol{\Sigma} = \mathbf{h}_0^{-1}(\mathbf{S} - p)\mathbf{h}_0'^{-1}\Omega_0. \tag{2.24}$$

In deriving Eq. (2.23) we have dropped inconsequential con-

stant terms in the energy viz. $p\Omega_0$ and $\Omega_0\,\mathrm{Tr}(\mathbf{S}-p)$. We have also used the identity $\mathrm{Tr}(\mathbf{AB}) = \mathrm{Tr}(\mathbf{BA})$.

Using Eq. (2.23) to write the Lagrangian equations of motion we get Eq. (2.9) as before but Eq. (2.10) is now replaced by

$$W\ddot{\mathbf{h}} = (\pi - p)\boldsymbol{\sigma} - \mathbf{h}\boldsymbol{\Sigma}. \tag{2.25}$$

It is easy to see that, analogous to Eq. (2.13), the Lagrangian $\mathscr{L}_s$ gives rise to a $(\mathbf{S}, H_s, N)$ ensemble where the generalized enthalpy is

$$H_s = E + V_{\mathrm{el}}, \tag{2.26}$$

where E is given by Eq. (2.14) and V_{el} by Eq. (2.20).

The equations of motion Eq. (2.25) imply that a state of equilibrium will necessarily give zero for the average value of the right side of Eq. (2.25). This makes, using the definition of $\boldsymbol{\Sigma}$, and writing $\boldsymbol{\sigma}_0$ for the equivalent of Eq. (2.7),

$$\langle(\pi - p)\boldsymbol{\sigma}\rangle = \langle\mathbf{h}\rangle\mathbf{h}_0^{-1}(\mathbf{S} - p)\boldsymbol{\sigma}_0. \tag{2.27}$$

This suggests, as is otherwise obvious intuitively, that for a system in equilibrium, to relate the constant matrix $\boldsymbol{\Sigma}$ [which controls the trajectories via Eq. (2.25)] to the external stress matrix $\mathbf{S}$ through Eq. (2.24), the most reasonable choice for the reference state appears to be $\mathbf{h}_0 = \langle\mathbf{h}\rangle$.

III. SUMMARY OF PREVIOUS STATIC CALCULATIONS

Before discussing our MD calculations in the next section and to put them in proper context, it is appropriate to recapitulate some of the results obtained by Milstein and collaborators.[3–5] In their model for Ni they assume a pairwise additive potential for the system, the pair potential being

$$\phi(r) = D\{\exp[-2\alpha(r - r_0)] - 2\exp[-\alpha(r - r_0)]\}. \tag{3.1}$$

The constants D, α, and r_0 are fixed from a fit to the elastic constants c_{11} and c_{12} and to the lattice constant a_0 of fcc nickel.[3] Using this potential, all the properties are calculated at zero temperature, starting with a perfect fcc arrangement. The details of the procedure to calculate the stress-strain relation are given in Ref. 5. We only recall that in these calculations the lengths a_1, a_2, and a_3 of the initially cubic cell are allowed to adjust to changing stress conditions, but the angles between the cell edges are constrained to remain right angles. Moreover, for each set of a_1, a_2, and a_3 values, the atoms are given appropriately modified lattice positions but of course without any thermal disorder. The results that are obtained by Milstein and Farber[5] are as follows, when the system is subjected to a homogeneous [100] load.

Along a " primary path" in the stress-strain relation (as indicated in Fig. 1) one has $a_1 \neq a_2 = a_3$ and along this path three structures can be identified at zero load (Fig. 1). One of the three obviously is the original undistorted fcc state for which $a_1 = a_2 = a_3 = a_0$. The second, $B^{(1)}$, is a bcc structure obtained in compression (i.e. $a_1 < a_0$) at $a_1 \simeq 0.80\,a_0$, $a_2 = a_3 = \sqrt{2}a_1$. The third, $T^{(1)}$, is a tetragonal state, also obtained in compression with $a_1 \simeq 0.75 a_0, a_2 = a_3 \simeq 1.59 a_1$. The fcc state is at the absolute minimum of energy, $B^{(1)}$ at a local maximum and $T^{(1)}$ at a local minimum.[5] From a consideration of the Born stability criteria one concludes[4] that $B^{(1)}$ and $T^{(1)}$ should be unstable states.

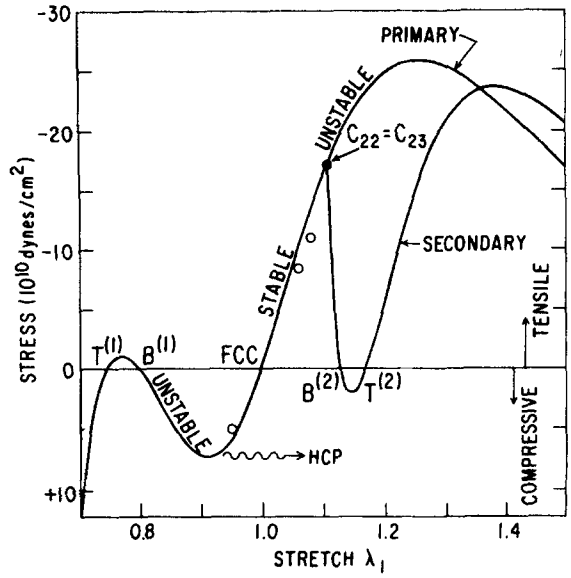

FIG. 1. Stress-strain relation under uniaxial load. O denote our results, lines are the static calculations of Milstein and Farber.[5] We found: (i) System failure at point (marked $c_{22} = c_{23}$) of intersection of the primary and secondary paths of Ref. 5; (ii) B and T tetragonal states on the zero load line spontaneously evolve into hcp structures; (iii) Under extreme compressive loading (marked by $\rightsquigarrow$) the system changes to an hcp structure.

Along the same "primary path" but when a_1 is increased under the action of a tensile load the system is predicted[4] to fail at a value of stress $= 16 \times 10^{10}$ dyne/cm^2 because at that point the Born stability condition $c_{22} - c_{23} > 0$ is violated. At this point $a_1 = 1.107\,a_0$.

However, it was discovered by Milstein and Farber[5] that at the point where $c_{22} = c_{23}$, a "secondary path" branches out of the primary path of extension. Along the secondary path, with decreasing load, the tetragonal symmetry is broken, i.e. $a_2 \neq a_3$ along this secondary path. This point, at which $c_{22} = c_{23}$, is hence a bifurcation point. Along the secondary path the zero load condition is encountered at two points where tetragonal symmetry is reestablished. One, a bcc state, $B^{(2)}$ at $a_1 = a_2 = \sqrt{2}a_3 = 1.1293\,a_0$ and the other a tetragonal state, $T^{(2)}$, with $a_1 = a_2 = 1.5701\,a_3 = 1.1696\,a_0$; $B^{(2)}$ is at a local energy maximum and $T^{(2)}$ at a local minimum.

The existence of this secondary path was envisaged in Ref. 5 as a possible mechanism for an fcc to bcc transition under conditions of a strictly uniaxial [100] tensile load.

IV. MOLECULAR DYNAMICS RESULTS

An MD calculation on Ni using the Lagrangian $\mathscr{L}_s$ of Eq. (2.23) makes it possible to check the validity of the results summarized above. This is because in MD with the Lagrangian $\mathscr{L}_s$ the restrictions of zero temperature and preassigned crystalline arrangement can both be removed.

As is customary we shall use reduced (i.e. dimensionless) quantities to specify various physical parameters. These reduced quantities will be denoted by an asterisk.

We shall use $D = 0.35059 \times 10^{-12}$ erg to be the unit of energy; $L = r_0/2^{1/6} = 2.2518$ Å that of length; m the mass of

the Ni atom, that of mass. Then $\tau = (mL^2/D)^{1/2}$ $= 0.375 \times 10^{-12}$ sec will be the unit of time. D and r_0 are the quantities occurring in the potential[3] Eq. (3.1). All calculations were made with $p^* = 0$, $W^* = 20$. (This choice of W^* is suggested by our previous experience[2] in using the Lagrangian $\mathscr{L}$). Since we were interested in static averages no attempt was made to calibrate W^* so as to obtain a realistic value for the relaxation times related with the behavior of Eq. (2.25). As discussed in Sec. 2 the choice of W^* only affects the calculation of dynamical correlations.

Throughout, we have monitored the structure of the system by calculating the pair correlation function $g(r)$ as was done previously.[2] In certain situations it was found useful to plot out all the particle coordinates in suitable two-dimensional "slices" of the three-dimensional system so as to get a visual impression of the structure.

Since the various MD calculations fall into distinct categories, these will now be identified through subsections and suitable subheadings.

A. Preparation of a system under conditions of zero stress

The genesis of this and all subsequent calculations was a 500-particle system of Ni atoms on a perfect fcc lattice. The initial value of $\mathbf{h}^*$ was $h^*_{ij} = 1^*_0 \delta_{ij}, 1^*_0 = 7.8244$. Hence the MD cell at the start was a perfect cube. A small random displacement of the particles from the lattice sites and zero velocities provided the initial conditions for the ensuing dynamics. The equations of motion, Eqs. (2.9) and (2.25), were solved, with $\Delta t^* = 0.01$, using the predictor-corrector algorithm.[11] For this calculation Σ was put equal to zero in Eq. (2.25). Initially the temperature of the system was controlled with the standard procedures of MD. After a long period of "aging" to allow for the establishment of equilibrium, an MD run was made in which the temperature fluctuated around the mean value $T^* = 0.14$ (i.e.350° K). The MD cell remained a cube to high accuracy (i.e., the nondiagonal elements of $\mathbf{h}$ fluctuated around essentially zero values). The mean value of the three cell edges was the same, being $1^*_{0.14} = 7.88 \pm 0.02$. The pair correlation showed an unmodified fcc structure.

B Compressive uniaxial loading

A configuration (i.e., the values and the derivatives of all the dynamical variables) of the equilibrium run just described was used as the initial condition for a calculation in which a uniaxial [100] compressive load was applied. In other words Σ^*_{11} was nonzero positive, all other Σ^*_{ij} being 0. Σ^*_{11} was raised to a value $\Sigma^*_{11} = 15$ using two short intermediate runs at $\Sigma^*_{11} = 4$ and 8. Under the action of such a load the matrix $\mathbf{h}$ starts to change in a very well defined manner, i.e., the MD cell starts to distort away from its initial cubic shape. As expected there is a contraction in the [100] direction and an expansion in [010] and [001] directions while preserving the tetragonal symmetry to high accuracy. At $\Sigma^*_{11} = 15$ a long run of 5000 Δt^* was made. All averages were calculated with the last 2290 Δt^* of this run. We found

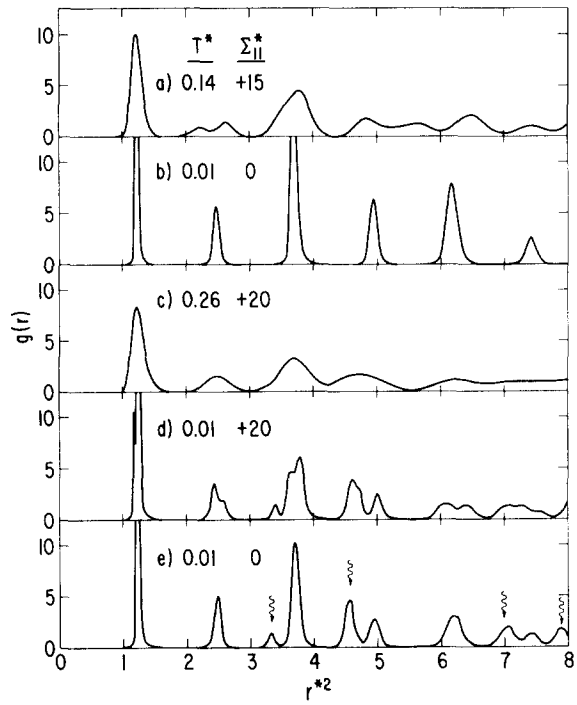

FIG. 2. Plot of pair correlation $g(r)$ to show structural transformation produced during compressive [100] loading. Note that abscissa denotes r^{*2} (not r^*). If r_i^* is the distance of the ith shell, r_i^{*2}/r_1^{*2} have the values 1, 2, 3, 4, 5, etc. for fcc and 1, 2, 8/3, 3, 11/3, 4, 5, etc. for hcp ordering. (a) Shows fc tetragonal structure at $\Sigma^*_{11} = 15$ (compressive [100] load) and $T^* = 0.14$. Note the splitting of the second peak corresponding to a "stretch" $\lambda_1 = 0.95$ (Sec. B). (b) System reverts back to fcc structure on unloading. Removal of thermal effects by quenching[12] to $T^* = 0.01$ shows perfect fcc shell structure (Sec. B). (c) At $\Sigma^*_{11} = 20$ large changes occur in the MD cell parameters (shown in Fig. 3). $g(r)$ shows some differences at large r; compare with (a) above (Sec. C). (d) At $\Sigma^*_{11} = 20$, after completion of structural changes, quenching reveals shells of hcp ordering in addition to peak splitting as in (a) above (Sec. C). (e) Unloading the system shown in (d) to zero load, letting it equilibrate at $T^* = 0.21$ then quenching the system leads to unambiguous shell structure of hcp ordering (Sec. C).

$\langle h^*_{11} \rangle = 7.45 \pm 0.05, \langle h^*_{22} \rangle = \langle h^*_{33} \rangle = 8.08 \pm 0.05$, giving a "stretch" $\lambda_1 = \langle h^*_{11} \rangle / 1^*_{0.14} = 0.95$. The nondiagonal $\langle h^*_{ij} \rangle$ were zero to within ± 0.05. Using $\langle \mathbf{h}^* \rangle$ for $\mathbf{h}^*_0$ one gets, from Eq. (2.24), $S_{11} = 5.25 \times 10^{10}$dynes/cm^2 for Ni, as seen in Fig. 1. This is in good agreement with the stress-strain relation given by Milstein and Farber.[5] (We note here that the nondiagonal elements of $\langle \mathbf{h}^* \rangle$ were so small as to be negligible; their inclusion or otherwise has no effect on the value quoted above for S_{11}).

The pair correlation of the system in equilibrium at $\Sigma^*_{11} = 15, T^* = 0.14$, is shown in Fig. 2(a). Note that $g(r)$, the pair correlation, is monitored as a function of $\mathbf{r}^2$; the second peak in Fig. 2(a) is split because the six original next nearest equidistant neighbors of the fcc structure break up into sets of two and four neighbors at slightly different distances. This splitting is not visible in the first peak because of thermal motion. The behavior of $\langle \mathbf{h}^* \rangle$ already made it clear that we had obtained a face-centered tetragonal structure. The $g(r)$ simply was a confirmation.

The fact that this equilibrium state under a uniaxial compressive load is reversibly connected to the original fcc

state was easy to demonstrate. Using the end of the above $\Sigma^*_{11} = 15$, $T^* = 0.14$ equilibrium run as the initial condition, the load was reduced to $\Sigma^*_{11} = 0$ in several short runs with successively smaller values of Σ^*_{11}, the temperature in the final $\Sigma^*_{11} = 0$ run being $T^* = 0.14$. Finally, on reaching a no load condition, the system was quenched to a very low temperature to observe the pair correlation with the effects of thermal motion removed.[12] This is shown in Fig. 2(b) leaving no doubt that one has regained the original perfect fcc structure. Of course, all other indicators, namely the components of $\mathbf{h}^*$, pointed to the same conclusion.

C. Structure transformation under further compression

After completing the $\Sigma^*_{11} = 15$ study the load was raised to $\Sigma^*_{11} = 20$ and the dynamics was allowed to take its course according to the dictates of the equations of motion [Eqs. (2.9) and (2.25)].

The behavior of the system was remarkably different as might have been guessed by the title given to this subsection. Figure 3 shows the details of the changes with the passage of time. The MD cell, i.e., the $\mathbf{h}$ matrix, undergoes large and swift changes which cannot possibly be described as elastic deformations. In fact, as Fig. 3 shows, when equilibrium was reached the average values of the components of $\mathbf{h}^*$ were $\langle h^*_{11} \rangle = 5.54 \pm 0.03$, $\langle h^*_{22} \rangle = 9.76 \pm 0.06$,

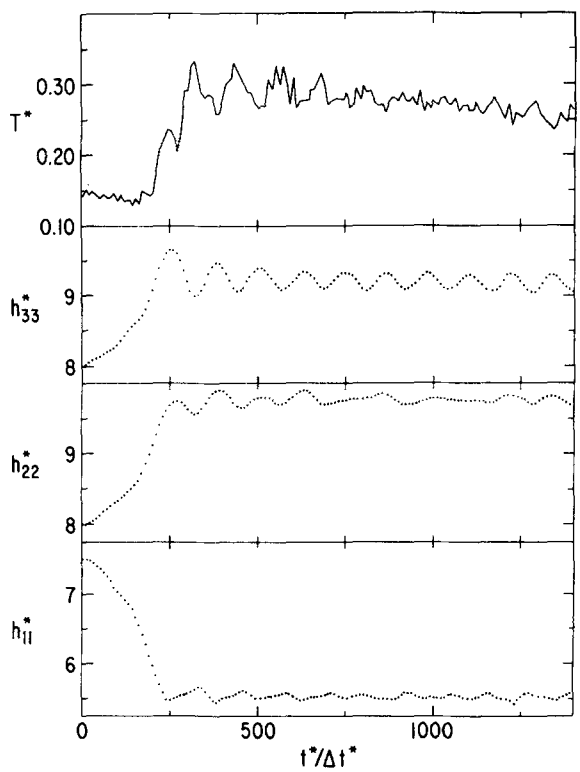

FIG. 3. Behavior of the MD cell parameters and the temperature of the system as it evolves in time when the compressive [100] load is increased from $\Sigma^*_{11} = +15$ to $+20$ (the latter value shown by $\rightsquigarrow$ in Fig. 1). After a rapid change h^*_{ii} settle down to values at which an hcp structure can be accommodated in the MD cell (Fig. 2(c) shows the $g(r)$ at the end of the above time elapse). The rise in temperature is due to the release of elastic energy as the transformation occurs. See Sec. C for details.

$\langle h^*_{33} \rangle = 9.18 \pm 0.09$. The average of the nondiagonal elements was essentially zero. We note here that the tetragonal symmetry of the initially stressed state is destroyed as a result of this transformation; one gets instead an orthorhombic system, still under [100] compression. (See below for the description of this orthorhombic system under zero load.)

As seen in Fig. 3, contemporaneously with the rapid changes in $\mathbf{h}^*$, the temperature T^* increased from ~ 0.15 to ~ 0.30, finally settling down to ~ 0.25 or perhaps somewhat less. This is obviously a manifestation of an abrupt release of elastic energy in the relatively short time interval of $\sim 100 \Delta t^*$ (or ~ 0.4 ps). Of course we recall that the $\Sigma^*_{11} = 15$ to 20 change was made in one Δt^*.

The pair correlation at the end of the $\Sigma^*_{11} = 20$ run is shown in Fig. 2(c). In spite of the large deformations in $\mathbf{h}$ mentioned above, the $g(r)$ in Fig. 2(c) is very similar to the one in Fig. 2(a) and does not show clear evidence of a new arrangement of particles. However, the quenching technique does indicate that a new structure has been formed. The $g(r)$ after quenching is shown in Fig. 2(d). This figure displays not only the shell structure of a hexagonal close packed system but it also shows that under this loaded state otherwise single shells show up as split into two. Visual examination of particle positions suitably displayed showed that stacking faults were present in the hcp arrangement. It is interesting to note here that the direction of the compressive stress is normal to the c axis of the new, close-packed structure.

Having obtained the above-described transformation under a compressive load we reduced the load from $\Sigma^*_{11} = 20$ to $\Sigma^*_{11} = 0$ using several intermediate steps. The temperature in the final $\Sigma^*_{11} = 0$ run was $T^* = 0.21$. There was no structural change evident during this process. To reveal the structure clearly at the end of this process (of reducing the load from a high value to zero) we used the usual quench technique. The $g(r)$ is shown in Fig. 2(e). The shell

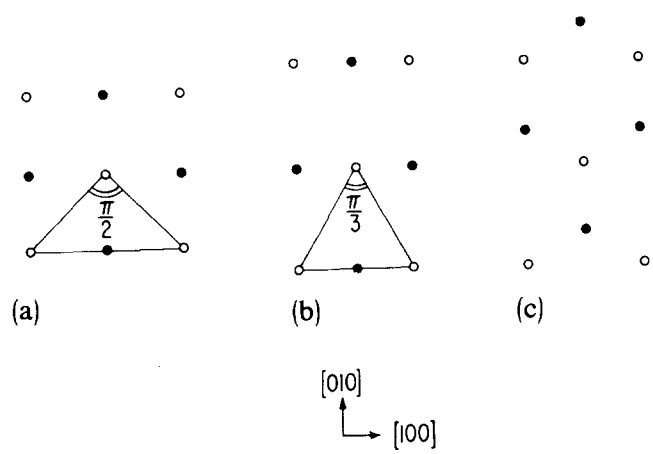

FIG. 4. Two planes of an fcc structure perpendicular to [001] are shown by ○ and ● respectively. (a)-(b) shows how the face-centered square structure changes to a triangular lattice on suitable compression in the [100] direction. (b)-(c) shows the necessary translation of the ● planes to achieve hcp ordering. At the same time spacing between ○ and ● planes has to correspond to the "c/a" value of an hcp arrangement, namely $\sqrt{8/3}$.

structure in Fig. 2(e) shows unambiguously an hcp arrangement. We recall that on reducing the load from $\Sigma^*_{11} = +15$ to $\Sigma^*_{11} = 0$ the system had gone back to its original fcc state (Sec.B 1).

The structure of the system which when quenched gave the $g(r)$ shown in Fig. 2(e) is of considerable interest. The distortions in the original cubic MD cell which allow an hcp structure to be accommodated were as follows: We found $\langle h^*_{22}\rangle/\langle h^*_{11}\rangle = \sqrt{3} \pm 0.01$, $\langle h^*_{33}\rangle/\langle h^*_{11}\rangle = \sqrt{8/3} \pm 0.01$, and an almost precise ($\langle h^*_{ij}\rangle \simeq 0.01, i \neq j$) rectangular parallelopiped. The ratio $\sqrt{3}$ is necessary to transform the [001] square-centered plains of the fcc structure into hexagonal plains [see Figs. 4(a)–4(b)]. The ratio $\sqrt{8/3}$ is the "c/a" value of the hcp structure. We note also that these distortions alone do not bring an fcc into an hcp structure; they have to be accompanied by the slip of alternate [001] planes as illustrated in Figs. 4(b)–4(c).

Given the highly coordinate nature of this transformation it is not surprising that in a rapid decompression defects such as stacking faults are produced.

D. System under tensile uniaxial loading

A study similar to the one just described was made by applying a tensile load; starting from the same configuration as was used to initiate the compressive runs, we raised the tensile load from 0 to $\Sigma^*_{11} = -20$ through a series of small intermediate steps at $\Sigma^*_{11} = -4, -8, -12, -16$. During these runs the MD cell remained tetragonal, elongated in the [100] direction and shortened equally in the [010] and [001] directions. At $\Sigma^*_{11} = -20$ the system was perfectly stable for the duration of a 4610 Δt^* MD run. During this run we obtained $T^* = 0.13$, $\langle h^*_{11}\rangle = 8.35 \pm 0.01$, $\langle h^*_{22}\rangle = \langle h^*_{33}\rangle = 7.75 \pm 0.02$, $\langle h^*_{ij}\rangle \simeq 0$ for $i \neq j$. The stress S evaluated from Eq. (2.24), using $\mathbf{h}^*_0 = \langle \mathbf{h}^* \rangle$, gave $S_{11} = -8.6 \times 10^{10}$ dyne/cm^2 for Ni, the strain, expressed as a stretch, being $\lambda_1 = \langle h^*_{11}\rangle / 1^*_{0.14} = 1.06$. These values are in complete accord with the results of Milstein and Farber[5] as seen in Fig. 1.

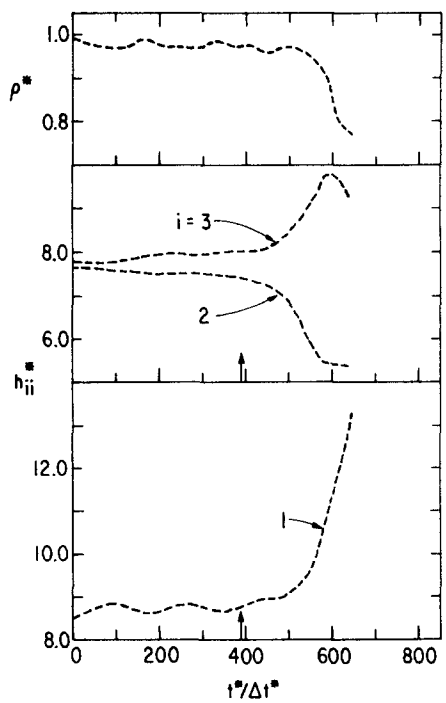

FIG. 5. At a tensile load of $\Sigma^*_{11} = -30$ the system fails after about 400 Δt. Initial breaking of tetragonal symmetry is clear ($h^*_{22} \neq h^*_{33}$). Arrow shows the critical moment after which even rapid unloading cannot prevent failure. Before the critical moment even slow unloading leads to the recovery of the original fcc state (see Fig. 1).

Increasing the tensile load to $\Sigma^*_{11} = -25$ gave a system like the one just mentioned. The final values were $T^* = 0.13$, $\langle h^*_{11}\rangle = 8.49 \pm 0.01$, $\langle h^*_{22}\rangle = \langle h^*_{33}\rangle = 7.72 \pm 0.04$, $\langle h^*_{ij}\rangle \simeq 0$ for $i \neq j$. This gave $\lambda_1 = 1.08$ and $S_{11} = -10.9 \times 10^{10}$ dyne/cm^2 again in accord with Ref. 5 as shown in Fig. 1. Note the proximity to the $c_{22} = c_{23}$ bifurcation point of Milstein and Farber.[5]

E. System failure under tensile uniaxial loading

On going from $\Sigma^*_{11} = -25$ to -30 the system "failed" as is described below. Figure 5 shows the values of h^*_{ii} as a function of time. The arrow indicates a region of time before which it has been found that it is possible to recuperate by rapidly reducing the load to more normal values. Beyond this time recovery may be difficult or impossible to achieve. This will be discussed in the following subsection.

As is clear from Fig. 5 the system does show a nontetragonal behavior at this increased load. This is in accord with the prediction of Ref. 5 regarding tetragonality in this region of strain, i.e., near the bifurcation point, made on the basis of static calculations. However, the fact of system failure really substantiates the conjectural remark of Milstein and Farber[5] that the very presence of the bifurcation point may lead to failure.

F. Recovery from failure

The configurations 100 Δt^* before and after the time indicated by the arrow in Fig. 5 were used as the initial conditions in a series of calculations at tensile loads smaller than the $\Sigma^*_{11} = -30$ value which leads to failure.[13] This was done in an attempt to capture, but without success, a stable point on the secondary stress-strain path of Milstein and Farber[5] i.e., a system without tetragonal symmetry.

In the first attempt, with a configuration occurring earlier than the position of the arrow in Fig. 5, Σ^*_{11} was brought to zero in a series of intermediate runs of about 300 Δt^* each (i.e., with slow unloading), with Σ^*_{11} reduced by five units every time. The final $\Sigma^*_{11} = 0$ state was found to be a system in which a cubic MD cell was reestablished; the structure had fallen back on to the undistorted fcc state of the primary path (see Fig. 1).

In the second attempt, with a configuration occurring later than the position of the arrow in Fig. 5, the length of the intermediate runs was 100 Δt^* (i.e., rapid unloading). Already at $\Sigma^*_{11} = -25$, i.e., during the very first intermediate run, the differences between h^*_{22} and h^*_{33} tended to increase monotonically. This tendency continued during the $\Sigma^*_{11} = -20$ run and the system failed.

We conclude that along the secondary path the system is unstable at high values of stress. As is shown in the next subsection *this is so even at zero load.*

G. Stable structures at zero load

As indicated in Sec. 3, the $B^{(2)}$ and $T^{(2)}$ states of Ref. 5 occur on the secondary path and at zero load. A calculation completely analogous to the one we reported[2] on a Lennard-Jones system was made on the Ni system now under consideration. Starting at $B^{(2)}$ i.e., with $h^*_{11} = h^*_{22} = \sqrt{2}\ h^*_{33} = 8.7826$, $h^*_{ij} = 0$ for $i \neq j, T^* = 0.11$ and $\Sigma^* = 0$, an MD calculation was initiated with the equations of motion given by $\mathscr{L}_s$ (which is the same as $\mathscr{L}$, because $\Sigma = 0$) of Eq. (2.23). The system spontaneously started to produce distortions in the MD cell and after only $890\,\Delta t^*$ the angles between the otherwise orthogonal axes became $\sim 89°$, $89°$, and $102°$ with an uncertainty of $\pm 3°$ in each case), the lengths of the edges of the MD cell became $1^*_1 \simeq 1^*_2 = 8.88 \pm 0.12$, $1^*_3 = 6.42 \pm 0.08$, while the temperature of the system rose to $T^* = 0.20$. These changes were accompanied by changes in the pair correlation function $g(r)$. As usual we quenched the system and this revealed a $g(r)$ corresponding to hcp ordering with stacking faults.

Instead of starting at the $B^{(2)}$ point, we started a calculation like the one described above from a configuration near the $T^{(2)}$ point on the secondary path of Ref. 5. This also transformed very fast to a system with hcp ordering with stacking faults. Note that the $T^{(2)}$ point is very little different from the $T^{(1)}$ state of the primary path. Since $T^{(1)}$ was found by Milstein[4] to be unstable it is not surprising that the same happens for $T^{(2)}$. Same remark applies a fortiori to the zero load bcc state since obviously it is the same state whether it is on one path or the other.

We did start a calculation from the $T^{(1)}$ state as the initial condition and, quite as we expected, the system evolved and gave an hcp state. In this case, the final state had no stacking faults.

We thus conclude that at zero load and finite (and rather low!) temperatures for Ni only the fcc structure is stable among the ones considered by Milstein and Farber.[5] However, as our calculations have clearly shown, a new, locally stable state is possible and this is an hcp structure.

The relative stability of the fcc and hcp structures is of course a difficult question to answer. An answer to this question requires a detailed and accurate computation of the free energy difference. From our calculations we can only infer that the local free energy minima in configuration space seem to be locally very stable at the low temperatures we have investigated.

V. CONCLUDING REMARKS

In this paper we have illustrated some of the possibilities opened up by our new MD method for the investigation of the elastic behavior of solids. Our calculations have reproduced results obtained by others using static methods.

In Fig. 1 we have displayed how the stress-strain relation in the system is in good agreement with the results of Milstein and Farber.[5] We can go even further to state that the departure of our results away from their static results is itself in the right direction since the system will be "softer" in the presence of thermal agitation; Fig. 1 shows this indeed to be so. However, because of its greater flexibility, the new method has allowed us to predict new results. A clear example of this is a genuine bifurcation point: the *fcc→hcp transition under compression*. In principle such a transition could have been predicted by static calculations[5] of Milstein and Farber if they had searched for *all* possibilities instead of restricting themselves to the case of face-centered tetragonal states. In an MD calculation the system follows a dynamical trajectory determined by well defined dynamical equations and is free to assume the crystal structure most suited to the interaction potential and the ambient conditions of temperature and stress. Being a fully dynamical method it even allows the study of the kinetics of temperature and stress induced transformations.

A few words of caution are in order especially if one wants to make comparisons with laboratory experiments. One limitation comes from the small system size and periodic boundary conditions used for the dynamical simulation. This probably reduces but certainly does not eliminate the occurrence of extended defects such as grain boundaries or dislocations; these defects play an important role in the plastic behavior of solids. This limitation is, however, not intrinsic and can be much reduced with the use of much larger MD systems. The possibility of creating extended defects probably accelerates the breakdown of the system under applied stress. Thus the tensile strength we have obtained ($S_{11} \sim 11 \times 10^{10}$ dyne/cm^2) is probably only an upper bound to the true value.

The second weakness of model calculations is the use of potentials like the one in Eq. (3.1). This potential is purely empirical without much justification from a microscopic point of view. Moreover, the normal state properties of crystalline systems are determined by values of the potential and its derivatives only at distances where the various neighbors are situated. The detail of the short-range repulsion probably plays a crucial role in the phenomena discussed in this paper and is not so well determined when one uses normal state properties of the crystal to determine the parameters of the empirical potential. Especially in Ni a proper account of the role of d-electrons may call for the use of many body forces in a more realistic calculation. This again is not a intrinsic problem with simulation methods.

Some of the conclusions reached in this paper are expected to be consequences only of the symmetry; as such they have a greater range of validity than the potential used in arriving at those conclusions. For instance it is possible that the fcc-hcp transition in a [100] compression is observable. Since the many-body terms in the "true" potential function are expected to be of short range their presence or absence cannot play a determining role in this particular structural transformation.

From the point of view of structural transformation in monotonic systems it will be most useful to have a systematic study of model systems with pair interactions of the type $1/r^m - 1/r^n$ when these systems are put under various forms

of external stress. Such calculations and also the ones we have presented are an exact consequence (apart from problems related with the numerical solutions of differential equations) of the potential function used. As such they serve the function of data for testing approximate theoretical models of the phenomena under investigation.

There is the intriguing possibility that the fcc-hcp transition might actually occur in Ni single crystals under extreme conditions of shock.

ACKNOWLEDGMENT

This work was supported by the U.S. Department of Energy.

APPENDIX A

The connection between the formal definition of the strains, Eq. (2.19), and that given in elementary textbooks[14] is as follows. Consider a reference state in which the MD cell is a rectangular parallelopiped with edges parallel to the Cartesian reference frame. In this case $\mathbf{h}_0$ is diagonal, the diagonal elements being the lengths of the three edges. In a distorted state the MD cell is given by $\mathbf{h} = \mathbf{h}_0 + \Delta\mathbf{h}$ say. Up to linear terms in $\Delta\mathbf{h}$, we find from Eq. (2.6),

$$\mathbf{G} = \Delta\mathbf{h}'\mathbf{h}_0 + \mathbf{h}_0'\Delta\mathbf{h} + \mathbf{h}_0'\mathbf{h}_0. \tag{A.1}$$

Using this in Eq. (2.19), due to the diagonal form of $\mathbf{h}_0$ we get

$$\epsilon_{ii} = (h_{ii} - h_{0,ii})/h_{0,ii}, \tag{A.2}$$

and for $i \neq j$

$$\epsilon_{ij} = 1/2(h_{ij}/h_{0,jj} + h_{ji}/h_{0,ii}). \tag{A.3}$$

Equation (A2) connects the diagonal terms of the strain to the length variation of the edges of the cell while Eq. (A3) gives the expected relation between the off-diagonal terms and the changes in the angles between the edges.

Up to order Δh, the volume change is given, as in Eq. (2.21), by $\Delta\Omega = \Omega_0 \operatorname{Tr} \epsilon$.

[1]E. R. Cowley, G. Jacucci, M. L. Klein, and I. R. McDonald, Phys. Rev. B **14**, 1758 (1976).
[2]M. Parrinello and A. Rahman, Phys. Rev. Lett. **45**, 1196 (1980).
[3]F. Milstein, J. Appl. Phys. **44**, 3825 (1973).
[4]F. Milstein, J. Appl. Phys. **44**, 3833 (1973).
[5]F. Milstein and B. Farber, Phys. Rev. Lett. **44**, 277 (1980).
[6]J. P. Hansen and I. R. McDonald, *Theory of Simple Liquids* (Academic, London, 1976).
[7]H. C. Andersen, J. Chem. Phys. **72**, 2384 (1980).
[8]W. G. Hoover, D. J. Evans, R. B. Hickman, A. J. Ladd, W. T. Ashurst, and B. Moran, Phys. Rev. A **22**, 1690 (1980).
[9]L. D. Landau and E. M. Lifshitz, *Theory of Elasticity* (Pergamon, Oxford, 1959).
[10]Note that in the definition of **S** through Eq. (2.20) we have adopted a certain sign convention: $\mathbf{S} = +p$ corresponds to a system under hydrostatic pressure p.
[11]A. Rahman, in NATO Advanced Study Institute Series: *Correlation Functions and Quasiparticle Interactions in Condensed Matter*, edited by J. W. Halley (Plenum, New York, 1978).
[12]This procedure, used systematically in Ref. 2, is extremely useful for the purpose of resolving peaks in $g(r)$ which otherwise would merge in neighboring peaks especially if the corresponding coordination numbers are very different. For example, in an hcp structure the third and the fouth shells are very close to each other with a population, respectively, of 2 and 18 neighbors.
[13]In an MD calculation the "failure" of a system is manifested by a monotonic change in the h_{ii} and in an obvious disruption of the shell-like structure of $g(r)$. A monotonic drop in the value of the density is simply a consequence of the behavior of the h_{ii}.
[14]C. Kittel, *Introduction to Solid State Physics* (Wiley, New York, 1968).